

# Hybrid Goldstone modes in multiferroics

S. Pailhès<sup>1</sup>, X. Fabrèges<sup>1</sup>, L. P. Régnault<sup>2</sup>, L. Pinsard-Godart<sup>3</sup>, I. Mirebeau<sup>1</sup>, F. Moussa<sup>1</sup>, M. Hennion<sup>1</sup>, and S. Petit<sup>1</sup>

<sup>1</sup> Institut Rayonnement Matière de Saclay, Laboratoire Léon Brillouin, CEA-CNRS UMR 12, CE-Saclay, F-91191 Gif-sur-Yvette, France

<sup>2</sup> Institut Nanosciences et cryogénie, CEA-Grenoble, DRFMC-SPSMS-MDN, 17 rue des Martyrs, F-38054 Grenoble Cedex 9, France

<sup>3</sup> Institut de Chimie Moléculaire et des Matériaux d'Orsay, Laboratoire de Physico-Chimie de l'Etat Solide, UMR CNRS 8182. Bât 410, Université Paris Sud. F-91405 Orsay Cedex, France

(Dated: October 29, 2018)

By using polarized inelastic neutron scattering measurements, we show that the spin-lattice quantum entanglement in multiferroics results in hybrid elementary excitations, involving spin and lattice degrees of freedom. These excitations can be considered as multiferroic Goldstone modes. We argue that the Dzyaloshinskii-Moriya interaction could be at the origin of this hybridization.

Spontaneous symmetry breaking is a powerful concept at the basis of many developments in physics, especially in condensed matter and high energy physics. The low symmetry phase is described by an order parameter associated with low energy and long wavelength excitations, restoring the original high temperature phase symmetry. These Goldstone modes [1] are nothing but longitudinal and transverse phonons in solids, or spin waves in magnets. In case of multiferroic materials, two order parameters, namely the ferroelectric polarization and the magnetization, coexist and are strongly coupled by a spin-lattice interaction [2, 3]. As a result of this entanglement, the multiferroic Goldstone modes are expected to be new spin and lattice hybrid excitations called electromagnons [4, 5, 6, 7]. While their existence has been theoretically predicted for a long time [8, 9], their dual nature as both spin and lattice excitations makes them challenging to observe and study experimentally. Due to their dipole electric activity, they first could be detected by optical measurements [4, 8, 9]: evidence for their existence has been recently reported in different orthorhombic multiferroics, namely *GdMnO<sub>3</sub>*, *TbMnO<sub>3</sub>* [10], *Eu<sub>0.75</sub>Y<sub>0.25</sub>MnO<sub>3</sub>* [11], *DyMnO<sub>3</sub>* [12], *YMn<sub>2</sub>O<sub>5</sub>* and *TbMn<sub>2</sub>O<sub>5</sub>* [13]. However, their magnetic counterpart is still not clearly evidenced. Moreover, as optical techniques probe the zone center, the shape of their dispersion and thus the underlying mechanism responsible for the hybridization, is still unknown. In this letter, we report polarized inelastic neutron scattering experiments performed on the particular case of hexagonal *YMnO<sub>3</sub>* to unravel the spin-lattice dual nature of these hybrid modes. Moreover, as neutron scattering allow a global survey of the reciprocal space, we report the dispersion of these hybrid modes throughout the Brillouin zone. This result is discussed in the framework of the dynamical magnetoelectric coupling theory, where the Dzyaloshinskii-Moriya interaction plays a central role.

*YMnO<sub>3</sub>* becomes ferroelectric below 900K, with an electric polarization along the *c*-axis, due to alternatively long and short yttrium-oxygen bonds (parallel to the *c*-

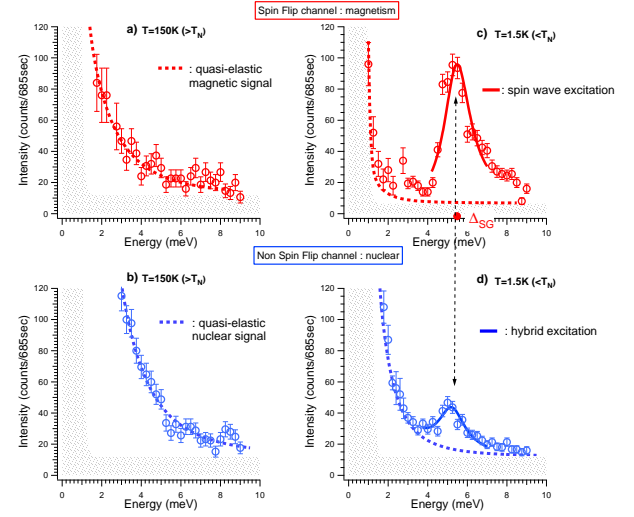


FIG. 1: (Color online) Dynamical magnetic and nuclear changes from the paramagnetic phase to the Néel ordered state. Figures (a) to (d) report energy scans in the SF (red labelled) and NSF (blue labelled) channels at the wave vector  $Q=(0,0,6)$  measured in the paramagnetic phase (left column) and in the Néel state (right column). Red and blue lines are fits to the data including the spin waves and the nuclear mode for low temperature scans.

axis) [14, 15]. Despite a strong geometric frustration, the Mn spin order below the Néel temperature  $T_N = 75K$  in a classical triangular arrangement [16, 17, 18] (Curie-Weiss temperature  $\theta = 500K$ ). The magnetic and electric order parameters strongly interact, as recently shown in reference [19], claiming the existence of a giant magneto-elastic coupling.

Through the comprehensive investigation of hybrid spin and lattice excitations, inelastic neutron scattering on a triple axis spectrometer combined with longitudinal polarization analysis (LPA) [20, 21] offer an efficient way to determine hybrid modes. Indeed, this technique allows to measure separately the spin-spin and nuclear-nuclear correlation functions in different channels (called

spin flip SF and non spin flip NSF respectively. It is worth noting that the magnetic cross section probes spin fluctuations perpendicular to the wave vector  $Q$  only. On the contrary, the nuclear cross section probes the atomic displacements parallel to  $Q$ . Measurements were carried out on the IN22 triple axis spectrometer at the Institute Laue Langevin (ILL, Grenoble, France). The sample was aligned in the scattering plane  $(100),(001)$  such that momentum transfer of the form  $Q=(H,0,L)$  in units of reciprocal lattice wave vectors were accessible and mounted into an ILL-type orange cryostat (1.5K-300K). All data were obtained with a fixed final wave vector of  $2.662\text{\AA}^{-1}$  providing an energy resolution less than 1meV. Heussler crystals were used as analyzer and monochromator, together with a flipper of Mezei to reverse the spin of the scattered neutrons. The elastic and inelastic measurement of the polarisation efficiency (flipping ratio), as determined from different magnetic Bragg peaks  $(100),(105),(003)$  and from the magnon signal at  $Q=(-0.4\ 0\ 6)$  and  $(1\ 0\ 1)$ , was of about 16 (elastic) and 14 (inelastic signal). The amplitude of the expected leak from the SF channel to the NSF channel is therefore less than 7% of the SF intensity. Using an unpolarized beam (PG monochromator), we measured a polarization parallel and perpendicular in- and out-of-plane to the wave vector less than  $10^{-2}$  excluding the presence of chiral terms and of the nuclear-magnetic interference terms [20, 21].

Energy scans at the wave vector  $Q=(0,0,6)$  in both channels measured above and below  $T_N$  are depicted on the panel B of the Figure 1. On the one hand, the strong magnetic quasi-elastic signal observed at 150K in the SF channel confirms the presence of strong spin-spin correlations in the paramagnetic phase arising from the geometrically frustrated Mn moments [16, 17]. Below  $T_N$ , 3 almost doubly degenerate spin wave modes are known to rise up [16, 22, 23]. At the zone centre, they are characterized by a spin gap  $\Delta_{SG}$ , typical of a magnetic anisotropy. Upon cooling below  $T_N$ , the magnetic long range order develops and  $\Delta_{SG}$  gradually shifts to higher values (Figure 2c), reaching its maximum of about 5.3 meV around 40K. On the other hand, the NSF intensity shows at 150 K a quasi-elastic signal as well. At 1.5K, the NSF data demonstrate the emergence of an additional inelastic nuclear mode. The energy of this mode coincides with the spin gap  $\Delta_{SG}$ , pointing out its close connection with the spin subsystem. To understand the temperature dependence of both quasi-elastic and inelastic modes, NSF energy scans have been performed at different temperatures around  $T_N$  (Figure 2a). From these NSF data, we extract the lattice susceptibilities, presented on Figure 2b. This analysis shows that the additional mode rises upon cooling on the top of the quasi-elastic signal as a supplementary intensity. Below 40K, the energy of this nuclear mode is found to follow the spin gap  $\Delta_{SG}$  (Figure 2c). Above 40K, its presence becomes

however hard to distinguish. To overcome this difficulty, we measured the NSF intensity at  $Q=(0,0,6)$  for sampling temperatures at 2.2 meV, well below the low temperature energy of the nuclear mode (Figure 2d). According to the above analysis, the quasi-elastic signal is expected to give a contribution proportional to the standard detailed balance factor (grey line). Figure 2 shows however subtle deviations from it in the intermediate region surrounding  $T_N$  (blue line), that we attribute to the raising of the nuclear mode starting from the lowest energies. These measurements allow estimating the energy of the nuclear mode for temperatures higher than 40K. Finally, we conclude that both spin gap and nuclear mode energies follow the same temperature dependence from 1.5 K till  $T_N$ . Since the nuclear cross section probes fluctuations along  $Q=(0,0,6)$ , which is parallel to the  $c$ -axis, we attribute the nuclear quasi-elastic signal to relaxational vibrations along this particular direction. The nuclear mode corresponds to collective vibrations along the same  $c$ -axis. Moreover, since it is found at a zone center, it corresponds to vibrations within the decoration of the unit cell. Now the question is: how do such internal motions propagate through the crystal?

To address this question, it is essential to determine the dispersion of the additional nuclear mode, by repeating the same measurements for different  $Q=(H,0,6)$  with varying  $H$  (Figure 3). We first determine the dispersion of the modes which are trivially expected, namely the spin wave modes (red points in SF channel on Figure 3) and the transverse acoustic phonon (denoted by P on Figure 3). Amazingly, the NSF data demonstrate unambiguously the existence of additional nuclear modes all along the low energy spin wave dispersions from  $Q=(0,0,6)$  to  $Q=(0.25,0,6)$  (denoted by HM on Figure 3). Their intensity is found to decrease as the wave vector increases. For instance, at  $Q=(0.325,0,6)$ , the nuclear intensity measured in the NSF channel becomes comparable to the expected leak of the intensity from the SF channel. Figure 3e evidences the fact that the dispersions of these nuclear modes match the spin wave dispersions for a wide range of wave vectors. It therefore appears obvious that they must be attributed to collective vibrations within the decoration that propagate through the crystal in the Néel state by hybridizing with the spin waves.

The discovery of a strong mixing down to the zone centre  $H=0$  shows that the long range properties of the system are affected. In explaining these findings, we thus propose to consider a coupling of the spin subsystem with atomic displacements within the unit cell [19]. This in turn implies a hybridization mechanism with an optical phonon, as in the dynamical magnetoelectric coupling theory developed for orthorhombic  $R\text{MnO}_3$  [4, 5, 24]. In this scenario, the spin current  $J_{ij} = S_i \times S_j$  (defined for neighbouring manganese spins  $S_i$  and  $S_j$  sitting at distance  $r_{ij}$ ) plays a crucial role. Owing to the

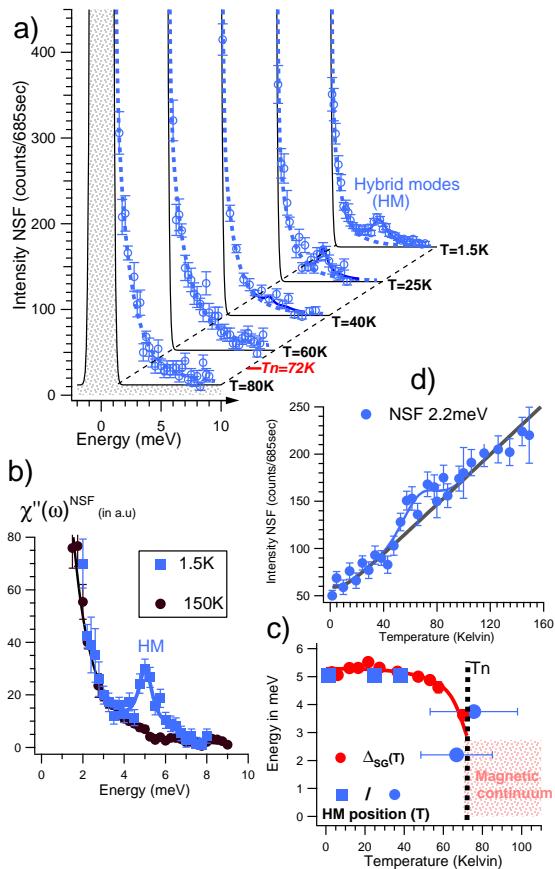


FIG. 2: (Color online) Nuclear mode at the zone center in the Nel phase. (a) Energy scans in the NSF channels at the wave vector  $Q=(0,0,6)$  for different temperatures above and below  $T_N$ . Below  $T_N$ , the additional nuclear excitation starts to form from the 40K (blue line). (b) Background subtracted and detailed balance factor divided intensity of (a). (c) Temperature dependences of the spin gap (red points, measured with unpolarized neutrons) and of the nuclear mode (blue points) positions. (d) Temperature dependence of the NSF inelastic intensity at 2.75 meV. The gray line corresponds to the detailed balance factor.

spiral magnetic ordering typical of these materials,  $J_{ij}$  acts, via the inverse Dzyaloshinskii-Moryia coupling, as a force pushing the oxygen atom located between adjacent manganese off the Mn-Mn bond. This mechanism gives rise at  $T_N$  to an electric polarization  $P = r_{ij} \times J_{ij}$  lying within the spiral plane and perpendicular to  $r_{ij}$ . The multiferroic Goldstone mode is predicted to be a hybrid mode, rising at  $\Delta_{SG}$ , and made of a mixing between the optical phonon associated with the oxygen displacement, and the spin wave mode involving spin fluctuations out of the spiral plane. At first glance, this mechanism would not hold in the hexagonal case, since due to the triangular symmetry, the resulting magnetic force experienced by oxygen atoms is zero: indeed, each oxygen ion is located at the centre of a triangle formed by 3 neighbouring Mn ions. The system can however benefit from

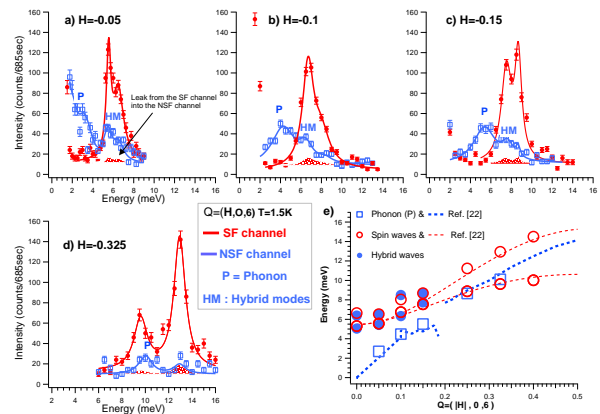


FIG. 3: (Color online) Nuclear and magnetic energy dispersions. Energy scans taken at 1.5K for different wave vectors  $Q=(H,0,6)$  in both SF (full points and red fits) and NSF (open points and blue fits) channels. The H component is indicated in the top left corner of each panel. The dotted line indicates the position of the nuclear mode (see text). The lowest right panel depicts the dispersions of the different low energy excitations: measured (filled red points) and calculated (dotted red lines) spin waves, transverse acoustic phonon6 (blue square) and hybrid modes (open blue circles).

the Dzyaloshinskii-Moryia interaction by spontaneously moving the oxygen atoms along the c-axis. This distortion is expected to create an electric polarization parallel to  $J_{ij}$  and is accompanied by a slight rotation of the spins towards the same direction. In that case, the coupled spin and atomic motions look like those of the ribs of an umbrella that would be put up or down (Figure 4). In close analogy with the orthorhombic case, hybridized spin-lattice Goldstone modes are expected at  $\Delta_{SG}$ , in agreement with the present results.

To test the validity of this scenario, several predictions have to be further examined. First, the magnetic structure should be characterized by a tiny ferromagnetic moment superimposed on the AF structure, as sketched in the right panel of Figure 4. In that case, specific Bragg peaks should exhibit a specific contribution at  $T_N$ . Calculations of the structure factor show that this effect is best observed for Bragg peaks with a forbidden AF magnetic intensity and a very weak nuclear one. The (2-11) Bragg peak fulfils these conditions. As shown on Figure 4, its intensity increases below  $T_N$ , and this is a good indication for the validity of this scenario. Next, as the high temperature ferroelectric distortion is mainly due to atomic displacements parallel to the c-axis, the oxygen displacements proposed in this umbrella scenario should result at  $T_N$  in a slight change of the ferroelectric moment. Evidence for such an evolution has been recently reported by Lee et al [19], thanks to high resolution X rays and neutrons diffractions measurements. This result is another argument supporting our interpretation.

In conclusion, polarized inelastic neutron scattering ex-

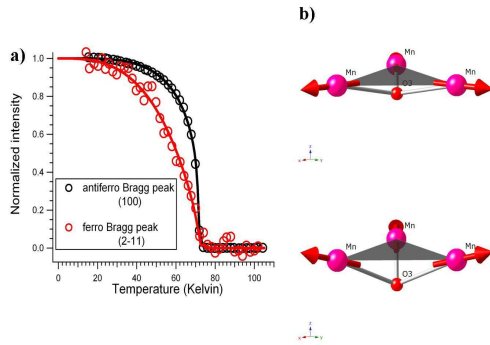


FIG. 4: (Color online) Umbrella scenario. Left figure (a) displays the temperature dependence of the (100) antiferromagnetic bragg peak and of the (2-11) Bragg peak (unpolarized neutron). The umbrella mechanism discussed in the text is sketched on the right panel (b). It evidences the existence of a small ferromagnetic component perpendicular to the Manganese (Mn)-Oxygen (O) layers when the oxygens are moving out of the plane.

periments demonstrate the existence of hybrid spin and lattice low energy modes in  $YMnO_3$ , that can be considered as Goldstone modes of the multiferroic phase. The neutron polarization analysis directly shows their hybrid nature, revealing both spin and structural counterparts. The mechanism responsible for this hybridization could be the Dzyaloshinskii-interaction, in close analogy with the model recently proposed for orthorhombic multiferroic materials.

We would like to thank Yvan Sidis, Martine Hennion and Fernande Moussa for fruitful discussions.

- [1] J Goldstone, Nuovo Cimento **19**, 154 (1961) and Phys Rev **127**, 965 (1962).
- [2] S-W Cheong, M. Mostovoy et al., Nature Materials **6**, 13 (2007)
- [3] J. F. Scott, Science **315**, 954 (2007)
- [4] H. Katsura et al., Phys. Rev. Letter **98**, 027203 (2007)
- [5] H. Katsura et al., Phys. Rev. Letter **95**, 057205 (2005)
- [6] M. Mostovoy, Phys. Rev. Letters **96**, 067601 (2006)
- [7] R. de Sousa, J.E. Moore, condmat/0706.1260v3 (2008)
- [8] V. G. Baryaktar and I.E. Chapius, Sov. Phys. Solid State **11**, 2628-2631 (1970)
- [9] I. A. Akhiezer and L. N. Davydov, Sov. Phys. Solid State **12**, 2563-2565 (1971)
- [10] A. Pimenov et al., Nature Physics **2**, 97 (2006)
- [11] R. Valds Aguilar et al., Phys. Rev. B **76**, 060404(R) (2007)
- [12] N. Kida et al., condmat/0711.2733 (2007)
- [13] A. B. Sushkov et al., Phys. Rev. Letters **98**, 027202 (2007)
- [14] Bas B. Van Aken et al., Nature Materials **3**, 164 (2004)
- [15] T. Katsufuji et al., Phys. Rev. B **66**, 134434 (2002)
- [16] T. J. Sato et al, Phys. Rev. B **68**, 014432 (2003)
- [17] J. Park et al, Phys. Rev. B **68**, 104426 (2003)
- [18] P.J. Brown and T. Chatterji, J. Phys. Cond. matter, **18**, 10085-10096 (2006).
- [19] Seongsu Lee et al., Nature **451**, 805 (2008), and Phys. Rev. B **71** 180413(R) (2005).
- [20] R. M. Moon et al., Phys Rev. B **181**, 920-931 (1969)
- [21] L. P. Regnault, Inelastic neutron polarization analysis, Neutron scattering from magnetic material, edited by T. Chatterji, Elsevier (2006)
- [22] S. Petit et al., Phys. Rev. Lett. **99**, 266604 (2007). The NSF data taken at  $H=0.15$  below and above  $T_N$  confirm the low temperature splitting of the phonons dispersion discussed in this reference.
- [23] T. Chatterji et al, Phys, Rev B **76**, 144406 (2007)
- [24] D. Senff et al., Phys. Rev. Lett. **98**, 137206 (2007)